

Intracellular number of magnetic nanoparticles modulates the apoptotic death pathway after magnetic hyperthermia treatment

Lilianne Beola,[±] Laura Asín,^{±,‡,} Catarina Roma-Rodrigues,[‡] Yilian Fernández-Afonso,[±] Raluca M. Fratila,^{±,‡} David Serantes,[†] Sergiu Ruta,[‡] Roy W. Chantrell,[‡] Alexandra R. Fernandes,[‡] Pedro V. Baptista,[‡] Jesús M. de la Fuente,^{±,‡} Valeria Grazú,^{±,‡} Lucía Gutiérrez^{±,‡,#,*}*

[±]Instituto de Nanociencia y Materiales de Aragón (INMA), CSIC-Universidad de Zaragoza, 50009 Zaragoza, Spain.

[‡]Centro de Investigación Biomédica en Red de Bioingeniería, Biomateriales y Nanomedicina (CIBER-BBN), Spain.

[#]Department of Analytical Chemistry, Universidad de Zaragoza, Edificio I+D, 50018 Zaragoza, Spain.

[‡]UCIBIO, Departamento de Ciências da Vida, Faculdade de Ciências e Tecnologia, Universidade Nova de Lisboa, Campus da Caparica, 2829-516 Caparica, Portugal.

[†]Applied Physics Department and Instituto de Investigacións Tecnolóxicas, Universidade de Santiago de Compostela, 15782 Santiago de Compostela, Spain.

[‡]Department of Physics, University of York, Heslington, YO10 5DD, York, United Kingdom.

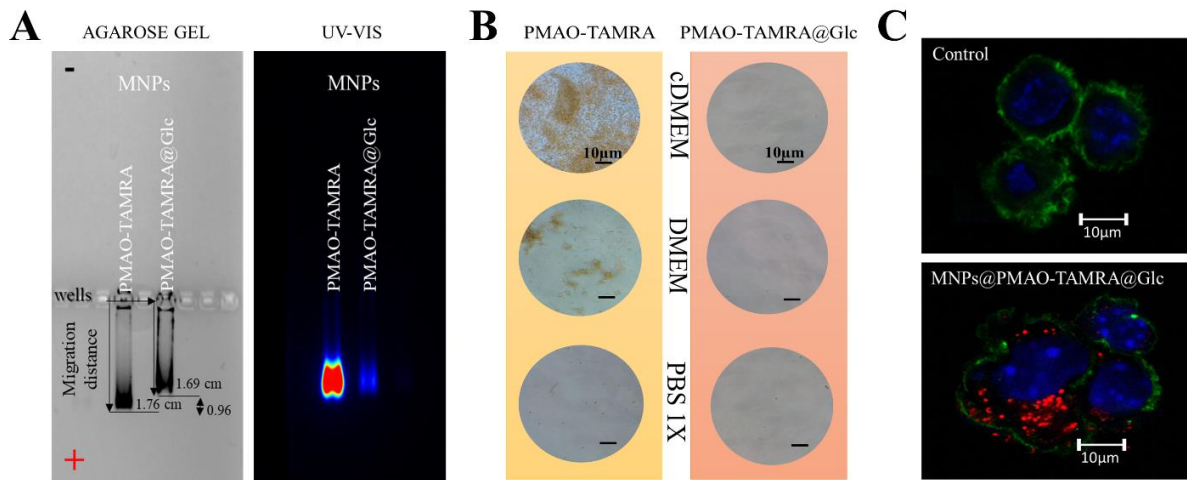
Figure S1: Characterization of the MNPs glucose functionalization efficacy

Figure S1. Characterization of the MNPs glucose functionalization efficacy (A) Agarose 1% gel image analysis and (B) stability study in different biological media - before (PMAO-TAMRA) and after (PMAO-TAMRA@Glc) glucose functionalization (C) Confocal images of the MNP uptake after Glc functionalization. The control image corresponds to cells without particles. The nucleus is shown in blue (DAPI), actin in green (PhalloidinAlexaFluor488), and MNPs in red (TAMRA). Scale bar: 10 μ m.

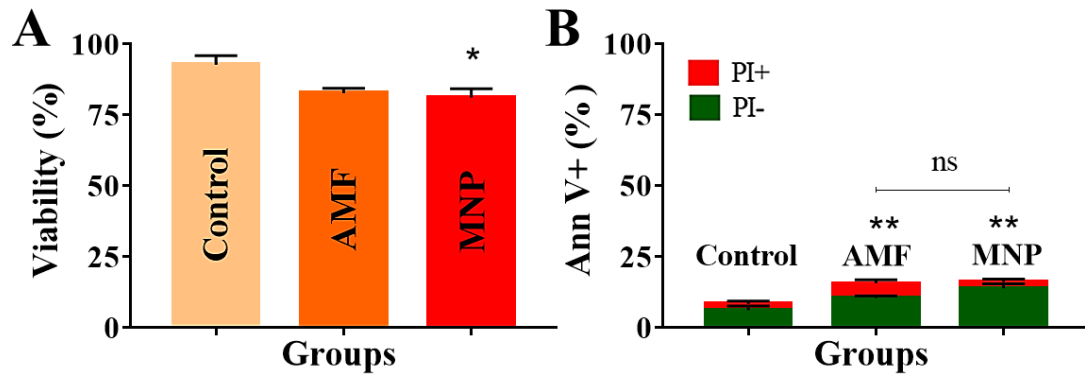
Figure S2. Cell viability studies

Figure S2. (A) Viability analysis and (B) Percentage of cells positive for Annexin V (+) that are either positive or negative for propidium iodide of the control samples from Figure 4C, D. Statistical significance between the means was determined using a one-way ANOVA followed of Dunnett's multiple comparisons test (A) and two-way ANOVA followed of Sidak's multiple comparisons test (B) (** $p < 0.01$; * $p \leq 0.05$; $p > 0.05$ no significance).

Figure S3: Hysteresis loop simulating the experimental conditions in water measurements

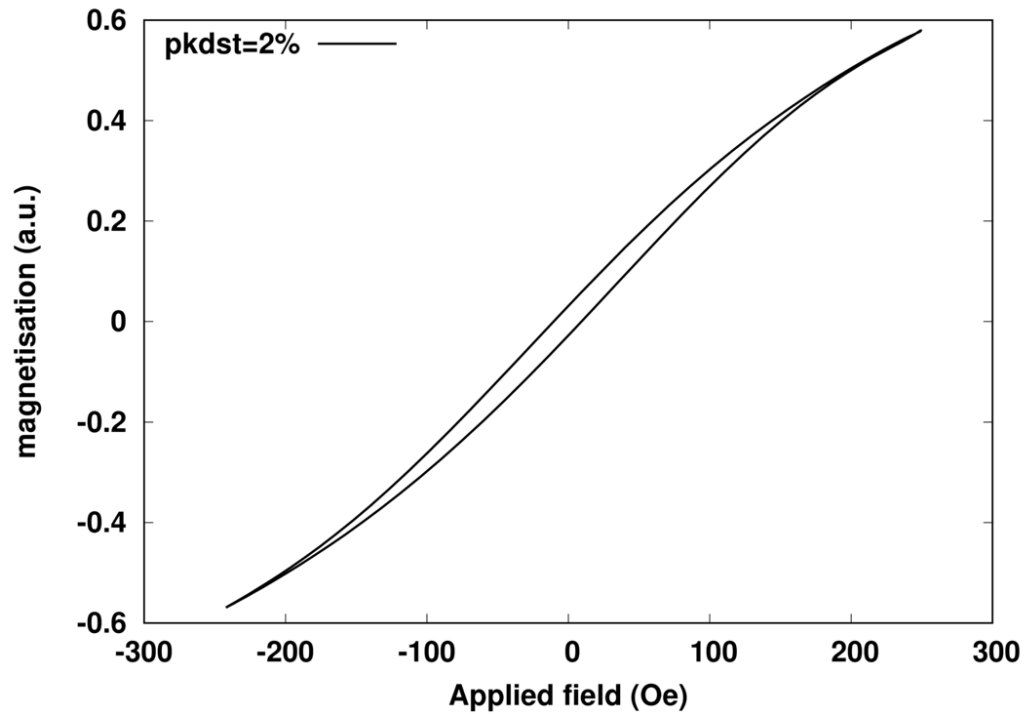


Figure S3: Hysteresis loop for anisotropy of $1.1 \cdot 10^4 \text{ J/m}^3$, applied field of 20 kA/m and frequency of 829 kHz at a low packing density of 2%.

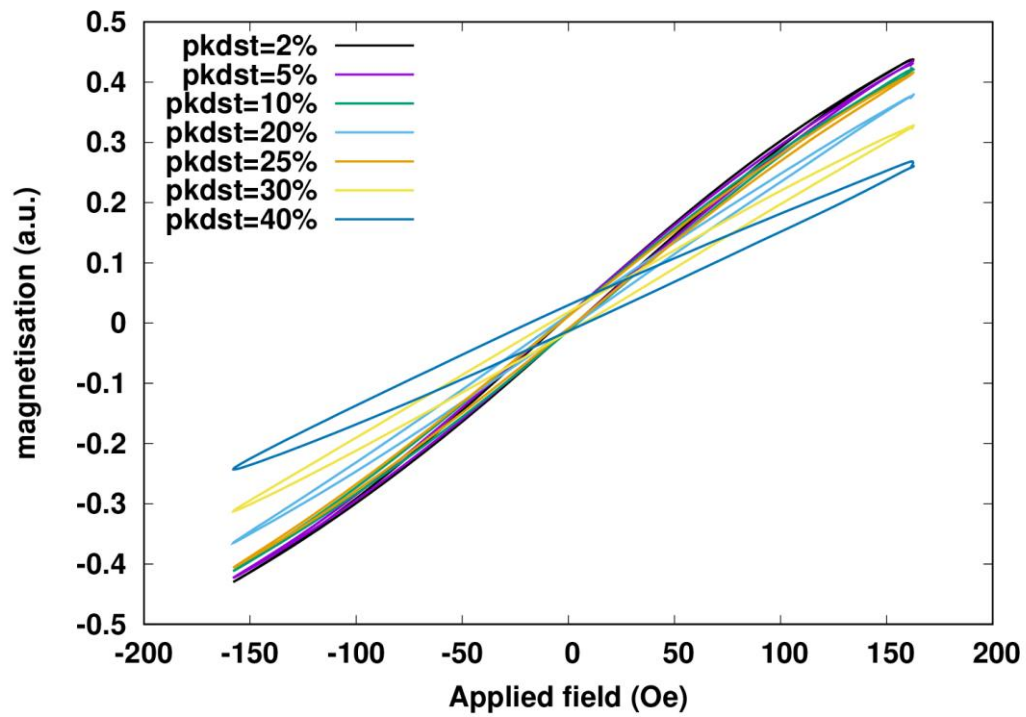
Figure S4: Hysteresis loops simulating the experimental conditions in vitro

Figure S4: Hysteresis loops at 379 kHz and applied field of 13 kA/m for different packing densities between 2% and 40%.

Computational details

To do the estimates of ΔT and $\Delta Q/S_{ly}$, we considered that the heat released by the particles during a certain time interval Δt , given by

$$\Delta Q_{MNP_s} = SAR \cdot \Delta t \cdot m_{MNP_s}, \quad (4)$$

with m_{MNP_s} the mass of the nanoparticles, results in an adiabatic temperature change of the entire system:

$$\Delta Q_{MNP_s} = c \cdot m_{TOT} \cdot \Delta T, \quad (5)$$

with c the specific heat capacity and m_{TOT} the total mass being heated. Depending on whether we consider each lysosome or the entire cell the containing system, different expressions for ΔT shall be obtained. Thus, if to begin with we consider that the system containing the particles during the adiabatic heating process is an isolated lysosome, then its temperature variation is given by

$$\Delta T_{lys} = \frac{SAR \cdot \Delta t \cdot m_{MNP_s}}{(c_{H_2O} \cdot m_{H_2O} + c_{MNP} \cdot m_{MNP_s})}, \quad (6)$$

using that $c \cdot m_{TOT} = c_{H_2O} \cdot m_{H_2O} + c_{MNP} \cdot m_{MNP_s}$, i.e. the total mass is that of the lysosome (associated with water parameters), plus that of the contained particles. Since we assume that the volume density of particles within the lysosomes is very similar for all lysosome sizes,

$$c = \frac{V_{MNP_s}}{V_{lys}} = 0.25. \quad (7)$$

It is convenient to rewrite Eq. (6) in terms of lysosome (water) and particles volume, using that $m_{MNP_s} = N \cdot \rho_{MNP_s} \cdot V_{1MNP}$ and $m_{H_2O} = \rho_{H_2O} \cdot V_{H_2O}$ (being N the number of particles within the lysosome, ρ_{MNP_s} (ρ_{H_2O}) the density of the particles (water), and V_{1MNP} and V_{H_2O} the volume of one particle and that of water within the lysosome, respectively). Using that $V_{lys} = V_{H_2O} + V_{MNP_s} = V_{H_2O} + N \cdot V_{1MNP}$, it is obtained that

$$m_{H_2O} = \rho_{H_2O} \cdot \left(\frac{1}{c} - 1 \right) \cdot N V_{1MNP} \quad (8)$$

This is to say, the fact that the volume concentration is always constant implies that both the mass of particles and that of the surrounding water within the lysosome are directly proportional to the number of particles N , so that Eq. (6) results in a size-independent ΔT :

$$\Delta T_{lys} = \frac{SAR \cdot \Delta t \cdot \rho_{MNP_s}}{\left(\frac{1}{c} - 1\right) \cdot c_{H_2O} \cdot \rho_{H_2O} + c_{MNP_s} \cdot \rho_{MNP_s}} \quad (9)$$

for the particular conditions of the present experiments, which results in close packing of the particles within the cells, the 2-nm thickness coating results in an effective volume fraction (of magnetic material) of about 25%, so that $(1/c-1)=3$, and $\Delta T_{lys} \approx 63$ K.

To estimate ΔT of the cell, ΔT_{cell} , we performed analogous reasoning but, in this case, taking in addition the total size of the cell (its average diameter, d_{cell}) as a key parameter. Thus,

$$\Delta T_{cell} = \frac{SAR \cdot \Delta t \cdot m_{MNP_s}}{c_{cell} \cdot m_{cell}}. \quad (10)$$

In this case $c_{cell} \cdot m_{cell} = c_{H_2O} \cdot m_{H_2O} + c_{MNP} \cdot m_{MNP_s}$, but since $m_{MNP_s} \ll m_{H_2O}$, we can safely approximate $c_{cell} \cdot m_{cell} \approx c_{H_2O} \cdot m_{H_2O} = c_{H_2O} \cdot \rho_{H_2O} \cdot V_{cell}$, resulting in

$$\Delta T_{cell} = \frac{SAR \cdot \Delta t \cdot N \cdot \rho_{MNP} \cdot d^3}{c_{H_2O} \cdot \rho_{H_2O} \cdot d_{cell}^3}, \quad (11)$$

with d and d_{cell} the average particle and cell diameters, respectively. In this case there is a clear dependence on the number of particles, as expected since the particle concentration per cell is different.

To estimate the heat flow per surface area of the lysosomes we followed similar reasoning. Firstly, using that $c = NV_{1MNP}/V_{ly}$, (with V_{ly} the lysosome volume), we write the average lysosome diameter in terms of the volume concentration,

$$d_{ly} = \left(\frac{6NV_{1MNP}}{\pi c}\right)^{\frac{1}{3}} = d \left(\frac{N}{c}\right)^{\frac{1}{3}}. \quad (12)$$

The surface area of the lysosomes, $S_{ly} = 4\pi(d_{ly}/2)^2$ can hence be written in general as

$$S_{ly} = \pi d^2 \left(\frac{N}{c}\right)^{\frac{2}{3}} \quad (13)$$

Now, using Eqs. (4) and (13), we directly obtain the energy flow per surface area of the lysosomes, $\Delta Q/S_{ly}$, as shown by Eq. (2) in the main text.

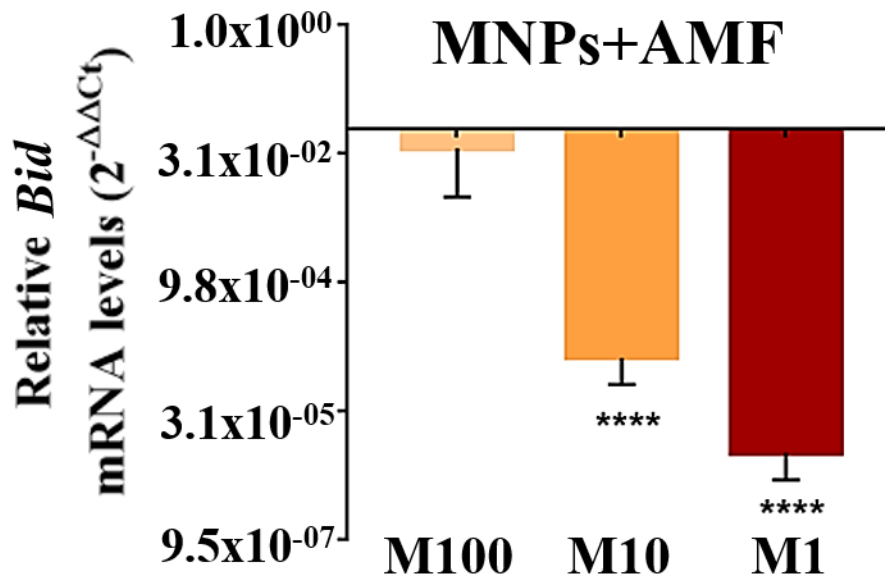
Figure S5. *Bid* expression analysis

Figure S5. Expression of *BID* mRNA 24 h after the exposure to AMF in the presence of different concentrations of MNPs (M10 to M100). Values were normalized to a control sample without MNPs (AMF). Statistical significance between the means was determined using a one-way ANOVA followed of Tukey's multiple comparisons test (**** $p < 0.0001$).